ELSEVIER

Nuclear Instruments and Methods in Physics Research A 405 (1998) 1–12

NUCLEAR INSTRUMENTS & METHODS IN PHYSICS RESEARCH Section A

Depolarization of dynamically polarized solid targets due to beam heating effects

T.J. Liu*,[1], T.D. Averett[2], D.G. Crabb, D.B. Day, J.S. McCarthy, O.A. Rondon

Department of Physics, University of Virginia, Charlottesville, VA 22901, USA

Received 6 November 1995; received in revised form 15 October 1997

Abstract

The behavior of dynamically polarized targets in the presence of a high intensity electron beam was studied. The nuclear polarization seen by the incident electron beam is lower than the overall measured target polarization by NMR due to beam heating and subsequent depolarization. A correction for this beam-induced depolarization is developed here to correct the measured target polarization for these effects. Furthermore, a model has also been developed to calculate the target depolarization in beam, and optimization of running conditions for future experiments of this nature are discussed based on this model.

Polarized nuclear targets have been used extensively over the past 30 years to investigate the role of spin in particle interactions. Recently, frozen $^{15}NH_3$ and $^{15}ND_3$ targets, working on the principle of Dynamic Nuclear Polarization(DNP) [1–3] were used in SLAC experiment E143 [4,5] to measure the proton and deuteron spin structure functions $g_1(x,Q^2)$ and $g_2(x,Q^2)$. For this experiment, a longitudinally polarized electron beam was scattered from target nucleons polarized either longitudinal or transverse with respect to the incident beam direction. The beam ranged in energy from 9.7 to 29.0 GeV and was delivered in 2.3 μs pulses at a rate of 120 Hz. As many as 4×10^9 e/pulse were incident on the target, making this highest beam intensity in which a solid polarized target has run in a routine manner. With such intense beams, the energy deposited has to be spread out to reduce the effect of depolarization due to increased temperature and radiation damage. If the beam is localized, the polarization can reduce rapidly and although the NMR measurement shows substantial polarization, the beam is traversing a region where the polarization maybe very small, thus compromising the experiment. The best way of spreading out the energy deposition is to raster the beam on the target in an appropriate manner, which greatly reduces local depolarization. However, rastering the beam does not automatically eliminate the difference between the NMR measured polarization and that seen by the beam. This paper estimates the size of this difference for

* Corresponding author: Tel.: +1 714 824 6444; e-mail: tjliu@uci.edu.

[1] Present address: Department of Physics & Astronomy, Univ. of California, Irvine, CA 92697, USA.

[2] Present address: Kellogg Radiation Lab, Caltech, Pasadena, CA 91125, USA.

0168-9002/98/$19.00
PII S0168-9002(97)01211-4

the E143 conditions and for other possible raster scenarios.

1. Beam heating corrections

The target material was in the form of solid beads/granules of radius ~ 0.7 mm held in a cylindrical container of radius 12.7 mm and length 3.0 cm. The entire assembly was immersed in a bath of liquid ^{4}He at a temperature of 1.1 K. We refer to Ref. [6] for details of the target cells and NMR operations. During E143, the beam was rastered over the face of the target in a circular pattern of radius 10.8 mm. For longitudinal polarization of the NH_3 target, the polarization dropped from an initial value of 75% with no beam present, to 68.3% when the beam was turned on at an intensity of 4×10^9 e/pulse. For longitudinal ND_3 running at the same beam intensity, the measured polarization dropped to 24.9%, from an initial value of 30%. When the beam was present, the target beads underwent large temperature and polarization changes, and so the polarization measured by the standard NMR technique [3,7,8], which samples the overall target polarization, is not necessarily the correct value seen by the beam. There are two sources which contribute to this difference:

1. The raster pattern only covers part of the target area. For the beads within the raster area, their temperature will increase due to beam heating, which subsequently causes an overall depolarization of the target material within the raster area. This effect will be discussed in full detail later. However, the beads outside of the raster area will remain at the temperature of the surrounding ^{4}He bath, and their polarization will not be changed from the original value.[3] The polarization measured by the NMR is a combination of both the unrastered beads and those which are in the raster region. The relative contributions from these two regions is sensitive to the geometry of the NMR coils and the radius of the raster pattern. Specifically, the relative contributions are weighted by the square of the perpendicular component of the RF magnetic field to the static magnetic field in the NMR system.
2. For the beads within the raster area, there is an additional temperature change due to the beam passing through them, and therefore their polarizations also fluctuate. As a result, the average polarization of the beads during the beam spill is not the same as that averaged over the entire raster period, which means that the average polarization that the beam sees is different from what contributes to the NMR signal. However, it will be shown later that this difference is very small and can be neglected in the present discussion.

We assume the relative contribution to the NMR signal from beads within the raster area is x, which is between 0 and 1. Assuming that the beads outside the raster area will remain at the initial (before beam) target polarization P_{init}, we have

$$P_{\text{meas}} = xP_{\text{T}} + (1 - x)P_{\text{init}}, \tag{1}$$

where P_{meas} is the measured polarizations once beam is turned on and the polarization has reached a steady state, and P_{T} is the true polarization of the rastered beads, see Fig. 1. Notice that P_{meas} is greater than P_{T} unless $x = 1$ (when the raster covers the entire target face), implying that the measured polarization is larger than the correct value. The above equation can be easily solved to yield

$$P_{\text{T}} = \frac{P_{\text{meas}} - (1 - x)P_{\text{init}}}{x}. \tag{2}$$

So to obtain the correct polarization, we need to multiply the measured polarization by a factor $(1 - C_{\text{heat}})$, where

$$1 - C_{\text{heat}} \equiv P_{\text{T}}/P_{\text{meas}}. \tag{3}$$

Because the NH_3 and ND_3 targets have different NMR coil geometries, and because the target $\boldsymbol{B}$ field changes direction relative to the NMR coils

[3] The ^{4}He bath temperature will actually rise when the beam is present. But the increase is as small as about 0.01 K, and translates into a negligible change in polarization.

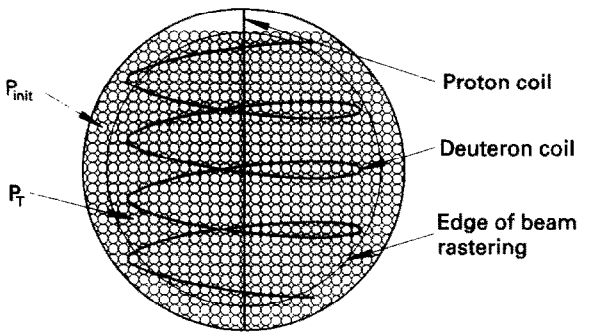

$$P_{meas} = xP_T + (1-x)P_{init}$$

$$1 - C_{heat} = P_T / P_{meas}$$

Fig. 1. Because the rastering does not cover the entire target cell, the polarization is different in the two regions. Incident beam is normal to the page.

for the longitudinal and transverse runs, the values for x and for C_{heat} will be different for each case. We denote the values of x as $x^h_{\parallel}, x^h_{\perp}, x^d_{\parallel}, x^d_{\perp}$ for NH_3 longitudinal and transverse runs, and ND_3 longitudinal and transverse runs, respectively. Once all four values for x are known, the corresponding correction factors can be readily calculated. Taking NH_3 as an example, for longitudinal runs we have $P_{meas,\parallel} = 68.3\%$ and $P_{init} = 75\%$, which allows us to solve for P_T. With P_T known, Eq. (3) immediately gives the value of C_{heat} for longitudinal runs. Transverse runs should have the same values of P_T and P_{init} as the longitudinal runs, so we have

$$P_{meas,\perp} = x^h_{\perp} P_T + (1 - x^h_{\perp}) P_{init} \quad (4)$$

and C_{heat} for the transverse runs can be similarly calculated.

To calculate the values for x, we note that the RF wavelengths of the NMR signals are much larger than the target cell dimensions so that a static field approximation can be used. The Biot–Savart law is used to calculate the magnetic field inside the target cell, yielding a value of x which is dependent on the geometry of the NMR coils. The target cell has radius 12.7 mm and length 3.0 cm, and the raster radius is 10.8 mm. The proton NMR coil is a straight vertical wire (oriented perpendicular to the static magnetic field of the target), and the deuteron coil is a four turn helical coil of diameter 17.0 mm and height 18.9 mm, with its axis oriented vertically. Also included in the model is the fact that the top 1.2 mm of the target cell is not filled with target material due to settling of the beads. The values of x and the correction factors in each case are shown in Table 1. To estimate the uncertainty in the correction factors, the values of raster radius R_{ras}, target settling depth L_{set}, the measured depolarization and the diameter of the ND_3 NMR coil D_{wire} were varied within reasonable limits, and the correction factors were re-calculated for each configuration. In this way, the corresponding changes give the size of error. The results are shown in Table 2.

Table 1
Beam heating correction results at beam intensity of 4×10^9 e/pulse

	$NH_3 \parallel$	$NH_3 \perp$	$ND_3 \parallel$	$ND_3 \perp$
P_{init} (%)	75	75	30	30
P_{meas} (%)	68.3	68.5	24.9	24.8
x	0.924	0.903	0.912	0.931
P_T (%)	67.7	67.7	24.4	24.4
C_{heat}	0.0081	0.0103	0.0197	0.0157

It was observed that the measured target depolarization ($P_{init} - P_{meas}$) is proportional to both the initial polarization (P_{init}) and the beam intensity. After plugging Eq. (2) into Eq. (3), it can be seen that the correction factors and their errors are independent of the value of P_{init}, but they scale with the beam intensity. The systematic errors on the NH_3 and ND_3 polarization measurements were 2.5% and 4% (relative) before these beam heating corrections were applied. However, due to the small errors in the correction factors, the overall errors in the target polarizations were essentially unchanged after the corrections were applied.

As an approximation, we have divided the target cell into two concentric circular regions where the inner circle sees beam uniformly while the outside sees none. Although a model with a smooth heating profile would be more realistic, it does not change

Table 2
Errors on the beam heating corrections at a beam intensity of 4×10^9e/pulse. The top table contains the x values for various configurations obtained by varying different parameters. The middle table contains the corresponding correction factors. The bottom table contains the errors on C_{heat} coming from varying parameters, where the row for P_{meas} contains the error coming from uncertainties in the measured polarization (absolute 0.6% for NH_3 and absolute 0.5% for ND_3). The sum is then combined with the relative systematic errors in the target polarization measurements obtained before the beam heating corrections

	$x^h_\parallel$	$x^h_\perp$	$x^d_\parallel$	$x^d_\perp$
Central value	0.924	0.903	0.912	0.931
$R_{ras}=10.5$ mm	0.900	0.874	0.893	0.914
$R_{ras}=11.1$ mm	0.941	0.923	0.931	0.946
$L_{set}=0.6$ mm	0.909	0.890	0.910	0.928
$L_{set}=1.8$ mm	0.941	0.919	0.917	0.935
$D_{wire}=16.0$ mm	—	—	0.923	0.939
$D_{wire}=18.0$ mm	—	—	0.900	0.920
	$C^h_\parallel$	$C^h_\perp$	$C^d_\parallel$	$C^d_\perp$
Central value	**0.0081**	**0.0103**	**0.0197**	**0.0157**
$R_{ras}=10.5$ mm	0.0110	0.0137	0.0245	0.0198
$R_{ras}=11.1$ mm	0.0062	0.0080	0.0152	0.0119
$L_{set}=0.6$ mm	0.0098	0.0118	0.0203	0.0163
$L_{set}=1.8$ mm	0.0062	0.0084	0.0185	0.0146
$D_{wire}=16.0$ mm	—	—	0.0171	0.0136
$D_{wire}=18.0$ mm	—	—	0.0228	0.0183
	$\delta C^h_\parallel$	$\delta C^h_\perp$	$\delta C^d_\parallel$	$\delta C^d_\perp$
R_{ras}	0.0029	0.0034	0.0048	0.0041
L_{set}	0.0019	0.0019	0.0012	0.0011
P_{meas}	0.0008	0.0010	0.0025	0.0019
D_{wire}	0	0	0.0031	0.0026
Subtotal	0.0036	0.0040	0.0064	0.0053
Error(rel) before	0.025	0.025	0.04	0.04
Error combined	0.025	0.025	0.04	0.04

the results. The diameter of the inner circle has been chosen as 10.8 mm based on the actual raster pattern and beam profile, by requiring the beam density at the edge to fall to half of its value at the center. The uncertainty in this diameter has been taken into account in the error estimate, and is small.

Another point worth noting is that the long-term target polarization depends on the total integrated radiation dose from the beam as well. In this model, we have assumed that the target beads inside the raster area have the same initial polarization as those outside. The justification is that the time scale for the radiation damage effect is several hours, which is much longer than that for the beam heating effect which is only a few minutes. The centroid of the beam raster pattern drifts slowly and randomly over time, so that on average, the whole target face is radiated uniformly. The drifting is fast enough as far as the radiation effect is concerned, so that at any given time, there is no significant difference between different parts of the target. On the other hand, it is also slow enough to be safely ignored as far as the beam heating effect is concerned. This effect is also reinforced by the fact that, the target beads also tend to drift within the target cell on a time scale comparable to the drifting of the beam centroid.

Finally, we note that these correction factors are within the systematic errors of the target polarization values.

2. Modeling the beam-induced depolarization

A model has been developed to calculate the target depolarization in beam. For simplicity, the focus is on the NH_3 target only. The relevant parameters for E143 are:

Beam current:	$4\times10^9\,e^-$/pulse
Beam energy:	29 GeV
Beam size:	1.4 mm diameter
Rastering pattern:	1.2 mm × 1.2 mm grid, over a 10.8 mm radius circle
Beam pulse rate:	120 pulses/s
Beam pulse length:	$t_{pul}=2.3\,\mu$s
Target material:	ammonia beads with average radius $r_{bead}=0.7$ mm.

There are a total of 253 raster positions, each occupied for one beam pulse so that in principle, a given raster point will not see beam again for 253 pulses. However, because the separation of adjacent raster points is smaller than the beam size, the effective time that the beam takes to come back is shorter. In a simplified model, we can think of an ammonia bead first being hit by the beam for one pulse, and then being hit again after $\pi\times(10.8\,\text{mm})^2/$

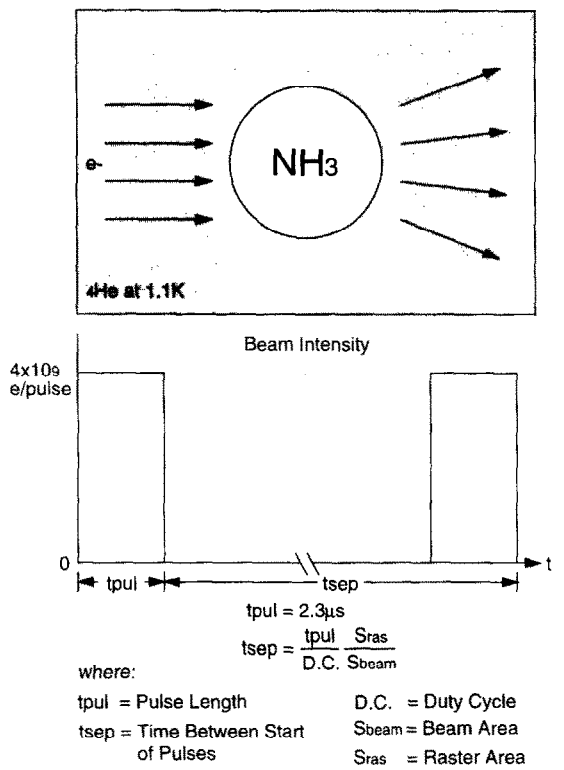

Fig. 2. Single ammonia bead model in beam.

$(\pi \times (0.7\,\text{mm})^2) = 238$ pulses (which corresponds to 1.98 s), as shown in Fig. 2. The variables t_{pul} and t_{sep} denote the pulse width, 2.3 μs, and the time the beam takes to come back to the same point, 1.98 s.

2.1. Polarization dependence of temperature with microwaves on

Dynamically polarized targets are polarized by the continuous application of microwave radiation. Here, we try to determine the maximum microwave-enhanced proton polarization as a function of temperature. First, look at the case where there are no microwaves present and the target is in thermal equilibrium with the surrounding liquid helium bath. From Boltzmann statistics we can write down the following expression for the thermal equilibrium polarization:

$$P_{te} = \tanh(\mu H/(kT_{\text{lattice}})), \tag{5}$$

where k is the Boltzmann constant, H the magnetic field, μ the magnetic moment of protons and T_{lattice} the lattice temperature. For protons at 5 T, $\mu H/k = 5.1084 \times 10^{-3}$ K. Similarly, the enhanced polarization with microwaves on is given by

$$P_{en} = \tanh(\mu H/(kT_{\text{spin}})), \tag{6}$$

where T_{spin} is the so-called "spin temperature" of the lattice. We assume the two temperatures are proportional:

$$T_{\text{spin}} = CT_{\text{lattice}}. \tag{7}$$

To find C, we assume a polarization of $P_{en} = 75\%$ at a T_{lattice} of 1.1 K, which is consistent with the E143 data. Using the above equation, we get $T_{\text{spin}} = 0.00525$ K, yielding $C = 0.00525/1.1 = 0.00477$. Using this value of C, we get

$$P_{\max}(T) = \tanh(\mu H/(kCT_{\text{lattice}})). \tag{8}$$

Fig. 3 is a plot of this function.

Next, we try to determine the polarization dependence with time t, at constant temperature T with microwaves on. We assume it approaches the maximum polarization exponentially, which means it takes the form

$$P(t) = P_{\max}(T)[1 - \exp(-\beta t - c)], \tag{9}$$

where β and c are independent of time t and the value of c is chosen to match the initial conditions.

The available data points at $T = 1$ K on polarization versus time with microwaves on are well fit by an exponential form. The fit gives $\beta = 0.2911/\text{min} = 0.004851/\text{s}$. This coefficient β represents how fast the maximum polarization is achieved, which depends on temperature T. We assume $(1/\beta)$ goes with T^{-4}, as does the temperature dependence of the lattice relaxation time, so $\beta(T) = 0.004851T^4$. We can setup an equation:

$$\frac{dP(t)}{dt} = \beta(T)[P_{\max}(T) - P(t)]. \tag{10}$$

We see immediately that as long as we have the temperature-dependence T with time t, we can solve the above equation and evaluate the polarization dependence. The first thing is to solve for $T(t)$.

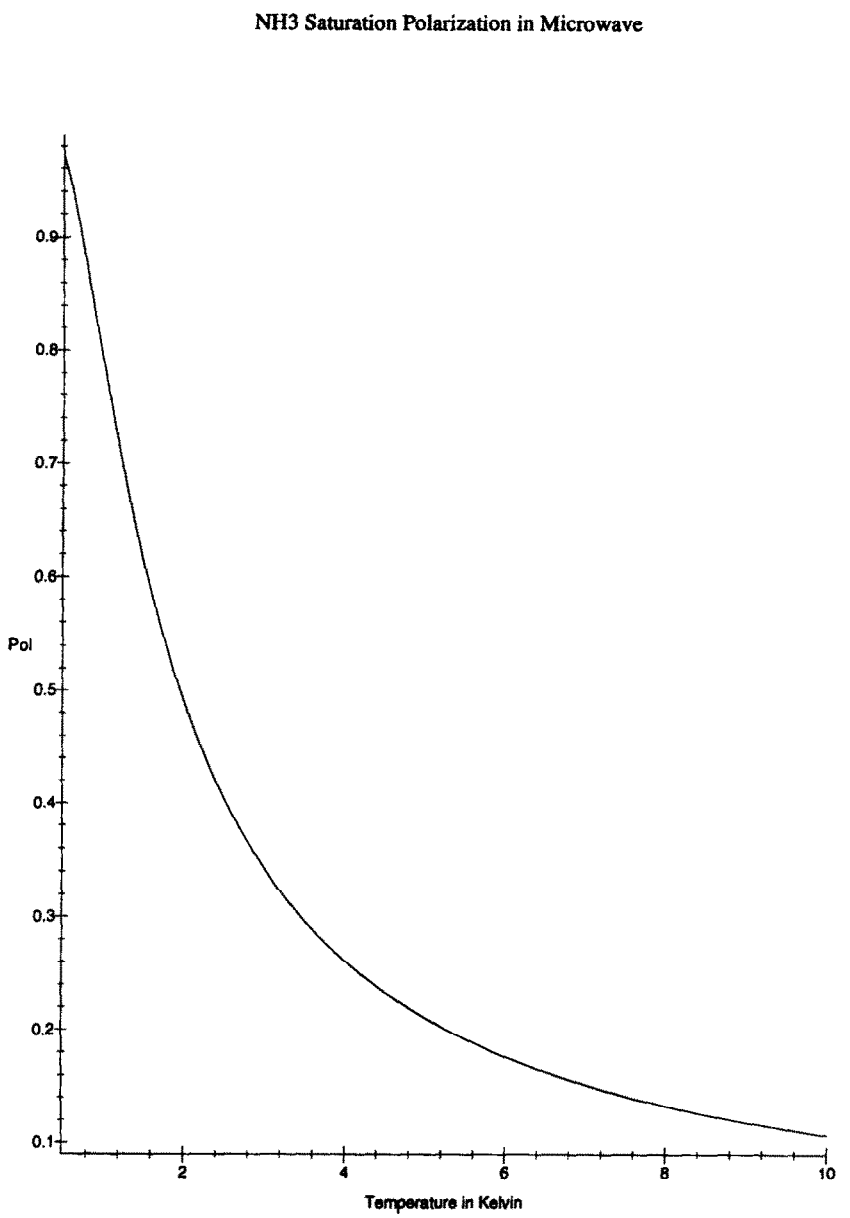

Fig. 3. NH_3 maximum polarization versus temperature.

2.2. *Target temperature variation in beam*

When an electron passes through a target, it loses energy by ionization and bremsstrahlung. The latter process dominates when the electron energy is large, as in this case. However, it is mainly the ionization loss that results in energy transfer into the target in the form of heat. For electrons in the energy range from 9 to 30 GeV, the ionization energy loss is approximately independent of the beam energy and may be taken as $2\,\mathrm{MeV\,g^{-1}\,cm^2}$. But because the electrons may be knocked out of the

target, the actual heat transferred to the target is less. Measurements of the heat transfer made at Mainz [9] indicate that roughly 60% of the ionization energy is actually deposited into the target and we therefore use a value of $1.2\,\mathrm{MeV\,g^{-1}\,cm^2}$. The following is a list of the thermal properties of NH_3 at low temperature, which were also obtained from Mainz:

Specific heat C_p:	$1.58\times10^{-4}\,\mathrm{J\,K^{-4}/Mol}T^3$ $=8.8\times10^{-6}\,\mathrm{J\,g^{-1}\,K^{-4}}T^3=C_{p0}T^3$
Thermal conductivity λ:	$2.3\times10^{-3}\,\mathrm{W\,cm^{-1}\,K^{-4}}T^3=\lambda_0T^3$
Kapitza alpha R_α:	$0.28\times10^{-2}\,\mathrm{W\,cm^{-2}\,K^{-4}}$ at 1.1 K
Density ρ:	$0.917\,\mathrm{g/cm^3}$

R_α is defined as [10]:

$$\frac{\text{heatflow}}{\text{area}}=R_\alpha(T^4-T_B^4), \tag{11}$$

where T_B is the bath temperature. A value of R_α was measured at Mainz and gave $2\times10^{-2}\,\mathrm{W\,cm^{-2}\,K^{-4}}$ at 1.1 K. This value has large uncertainties and is valid only for small temperature deviations. Using this original value, the calculated depolarization for NH_3 is smaller than what was observed. For this calculation, we use a value of $0.28\times10^{-2}\,\mathrm{W\,cm^{-2}\,K^{-4}}$ which is obtained by matching the calculation with our observed data.

At a beam intensity of $4\times10^9\,\mathrm{e^-/pulse}$, the heat deposited in one bead during one beam pulse becomes

$$\begin{aligned}\Delta E &= 1.2\,\mathrm{MeV\,cm^2/g}\times4\times10^9\times\tfrac{4}{3}\rho r_{\mathrm{bead}}\\ &= 1.2\,\mathrm{MeV\,cm^2/g}\times4\times10^9\\ &\quad\times\tfrac{4}{3}\times0.917\,\mathrm{g/cm^3}\times0.7\,\mathrm{mm}\\ &= 6.6\times10^{-5}\,\mathrm{J}.\end{aligned} \tag{12}$$

So the heating power per unit volume during the spill is

$$\begin{aligned}\dot{Q} &= 6.6\times10^{-5}\,\mathrm{J}/(\tfrac{4}{3}\pi(0.07\,\mathrm{cm})^3)/2.3\,\mu\mathrm{s}\\ &= 2.0\times10^4\,\mathrm{W/cm^3}.\end{aligned} \tag{13}$$

Beam heating of the target has two effects. First of all, it will raise the ^{4}He bath temperature. This effect is very small as confirmed by the ^{4}He and ^{3}He manometer readings during the experiment. Thus, a constant bath temperature of $T_B = 1.1\,\mathrm{K}$ is assumed. Second, the bead temperature will be higher than that of the bath, and will vary with time. A rough estimate of the temperature rise of one bead after the beam pulse can be made by assuming that there is no heat transfer from the bead to the bath. The mass of one bead is $m = \frac{4}{3}\pi(0.07\,\mathrm{cm})^3\times0.917\,\mathrm{g/cm^3} = 1.3\times10^{-3}\,\mathrm{g}$, so the final temperature T after the beam pulse is given by

$$\begin{aligned}&\tfrac{1}{4}\times1.3\times10^{-3}\,\mathrm{g}\times8.8\times10^{-6}\,\mathrm{J\,g^{-1}\,K^{-4}\,T^4}\\ &=6.6\times10^{-5}\,\mathrm{J}\end{aligned} \tag{14}$$

which gives $T = 12.3\,\mathrm{K}$. For a more accurate estimate we setup a Fourier equation, in which we assume spherical symmetry as an approximation so that the temperature T of the bead is only a function of radius r and time t. The equation is

$$\rho C_p\frac{\partial T}{\partial t}=r^{-2}\frac{\partial}{\partial r}\left(\lambda r^2\frac{\partial T}{\partial r}\right)+\dot{Q} \tag{15}$$

with the boundary condition

$$R_\alpha[T(r_{\mathrm{bead}},t)^4-T_B^4]=-\lambda\frac{\partial T}{\partial r}\bigg|_{r=r_{\mathrm{bead}}} \tag{16}$$

where ρ is the bead density, $\dot{Q}$ is the heating power of beam on the beads per unit volume. First, consider the equilibrium case when $\partial T/\partial t = 0$. Then the time-dependence drops out and the above equation reduces to

$$\rho C_p\frac{\mathrm{d}T}{\mathrm{d}t}=r^{-2}\frac{\mathrm{d}}{\mathrm{d}r}\left(\lambda r^2\frac{\mathrm{d}T}{\mathrm{d}r}\right)+\dot{Q}=0 \tag{17}$$

with the same boundary condition. Assuming λ to be constant, this equation can be solved to yield

$$T(r)=-\frac{\dot{Q}}{6\lambda}r^2+\frac{\dot{Q}}{6\lambda}r_{\mathrm{bead}}^2+\left(\frac{\dot{Q}r_{\mathrm{bead}}}{3R_\alpha}+T_B^4\right)^{1/4}. \tag{18}$$

Computing the quantity $(T(r_{\mathrm{bead}})-T_B)/(T(0)-T(r_{\mathrm{bead}}))$ we have

$$\frac{T(r_{\mathrm{bead}})-T_B}{T(0)-T(r_{\mathrm{bead}})}$$

$$= \left(\left(\frac{\dot{Q}r_{\text{bead}}}{3R_x} + T_B^4\right)^{1/4} - T_B\right) \Big/ \left(\frac{\dot{Q}}{6\lambda} r_{\text{bead}}^2\right)$$

$$= \left(\left(\frac{\dot{Q}r_{\text{bead}}}{3R_x} + T_B^4\right)^{1/4} - T_B\right) 6\lambda \Big/ (\dot{Q}r_{\text{bead}}^2)$$

$$> \left(\left(\frac{\dot{Q}r_{\text{bead}}}{3R_x} + T_B^4\right)^{1/4} - T_B\right) 6\lambda_{1.1\,\text{K}} \left(\frac{\dot{Q}r_{\text{bead}}}{3R_x} + T_B^4\right)^{3/4} \Big/ (\dot{Q}r_{\text{bead}}^2)$$

$$\equiv F(\dot{Q}), \tag{19}$$

where $\lambda_{1.1\,\text{K}}$ is the value of λ at $T = 1.1$ K, and the inequality comes from the fact that λ is an increasing function of T and the average T inside the volume is greater than the bath temperature. Putting in the value of all the parameters at $T_B = 1.1$ K, we find $F(\dot{Q}) \gg 1$, which suggests that the temperature variation within the bead is small compared with the drop at the surface. So, as a good approximation, assuming that the temperature is constant within the bead, and labelling it as $T(t)$, we can setup a differential equation

$$\frac{4}{3}\pi r_{\text{bead}}^3 \rho C_p \frac{dT}{dt} = \frac{4}{3}\pi r_{\text{bead}}^3 \dot{Q} - 4\pi r_{\text{bead}}^2 R_x (T^4 - T_B^4) \tag{20}$$

which simplifies to

$$C_{p0} \rho T^3 \frac{dT}{dt} = \dot{Q} - R_x \frac{3(T^4 - T_B^4)}{r_{\text{bead}}}. \tag{21}$$

Using the corresponding values, the above differential equation can be solved with the initial condition $T(0) = 1.1$ K. $\dot{Q}$ is taken to be 2.0×10^4 W/cm^3 for the first 2.3 μs, zero for the following 1.98 s, and it then repeats itself. The above equation can be parametrized to give

$$aT^3 \frac{dT}{dt} = b - c(T^4 - d^4) \tag{22}$$

with the initial condition that $T = T_0$ at $t = t_0$, where a, b, c and d are known constants. It has the following solution:

$$T = \left(\frac{1}{c}\left(b + cd^4 + \exp\left(-\frac{4(t - t_0)c}{a}\right) \times (cT_0^4 - b - cd^4)\right)\right)^{1/4}. \tag{23}$$

Substituting in the values of a, b, c, d with $t_0 = 0$ at $T_0 = 1.1$, we get the solution of T for the first 2.3 μs, which gives $T = 12.1$ K at $t = 2.3$ μs. Then, for $2.3\,\mu\text{s} < t < 1.98$ s, substituting $b = 0$ into the above equation, we get

$$T = \left(d^4 + \exp\left(-\frac{4(t - t_0)c}{a}\right)(T_0^4 - d^4)\right)^{1/4}. \tag{24}$$

with the initial condition $T_0 = 12.1$ (K) at $t_0 = 2.3 \times 10^{-6}$ (s). The overall temperature profile in one cycle is shown in Fig. 4. Notice that after the beam is gone, T stays at high temperature for about 0.1 ms, then goes down to the bath temperature. For $t > 1.98$ s, the periodic function T simply repeats itself.

Note that we have used a value of R_x which is different from that measured at Mainz. In fact, because of the large temperature excursions in a bead, the heat transfer may move from the nucleate boiling regime to the film boiling regime. In this case, the use of Eq. (11) is not appropriate. The difference between the value of R_x measured at small temperature deviations and the fitted one is

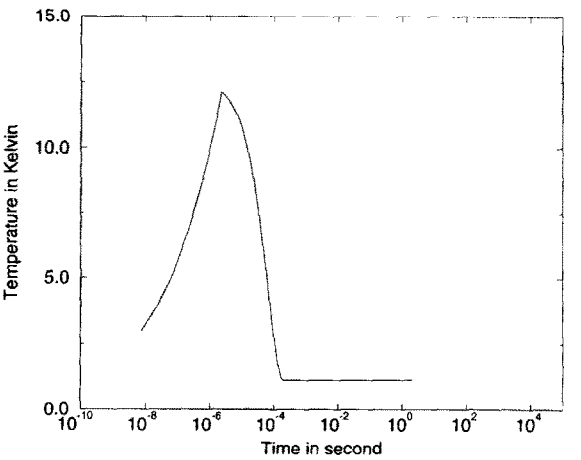

Fig. 4. NH_3 bead temperature variation in beam. Beam comes at time $t = 0$ and goes away after 2.3 μs.

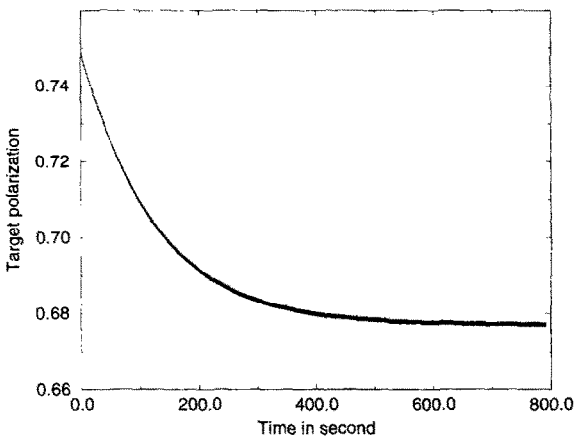

Fig. 5. NH_3 bead depolarization when beam turned on at time $t = 0$.

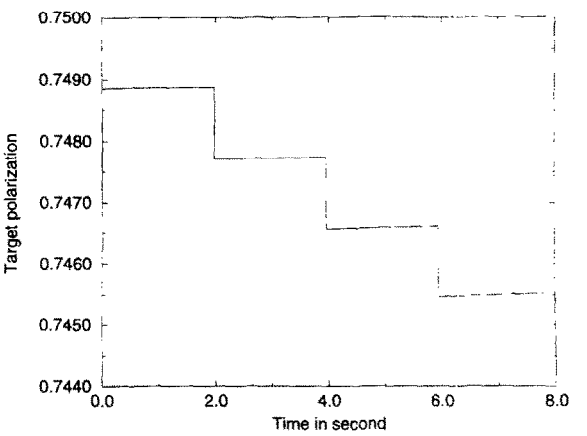

Fig. 6. Early stage of NH_3 bead polarization drop after beam turned on.

likely evidence for such a transition. However, we stress that, the general temperature and polarization profile are not altered by such considerations.

2.3. Depolarization calculation

Now, the depolarization effect can be calculated using Eq. (10). Now that the time dependence of T is known, $B(T)$ and $P_{max}(T)$ both become known functions of t. Eq. (10) has the following solution:

$$P(t) = e^{-\int_0^t B\,dt} \int_{t0}^{t} BP_{max} e^{-\int_0^t B\,dt}\,dt + P_0 e^{-\int_0^t B\,dt} \quad (25)$$

with the initial condition that $P = P_0$ at $t = t_0$. The solution of the above equation is shown in Fig. 5. With beam on, the initial target polarization of 75% drops off for the first 10 min or so, and then oscillates around 67.7%. Fig. 6 is a magnified view of the initial polarization behavior, and Fig. 7 is a magnification of the region where the polarization settles down. These figures show that as the polarization drops, the total amount of depolarization in one cycle does not change much when the bead temperature is high. This is because the material tends to depolarize exponentially to a relatively low polarization value, and a small drop in polarization does not significantly change the slope of the depolarization curve which determines how fast it depolarizes. During the rest of the cycle when

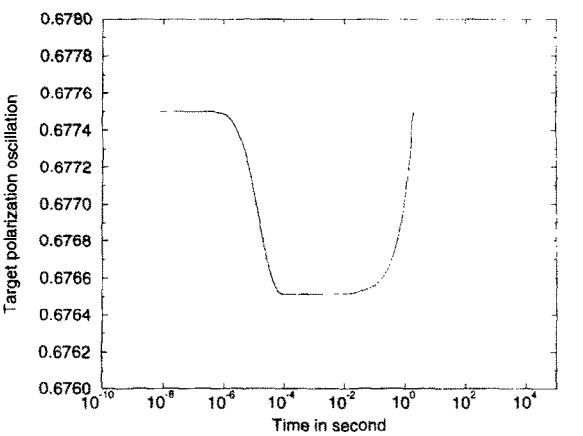

Fig. 7. NH_3 bead polarization variation in one cycle after settling down.

the bead temperature has cooled down close to that of the surrounding ^{4}He bath, it attempts to polarize back to the original 75% polarization and the slope gets steeper as it gets further away from the original value. Hence, the average polarization in each cycle continues to drop until the latter process is able to compensate the former. The average target polarization during the beam pulse is calculated to be 67.748% (this is what beam really sees), and over the entire period, the average polarization is 67.701% which is slightly less [this is P_T in Eq. (1)]. The ratio of them is 1.0007 which is very close to 1, which justifies treating the two quantities as equal

previously. For different beam intensities, calculations show that the depolarization ($P_{init} - P_{meas}$) approximately scales with the beam intensity.

3. Optimization of running conditions from the model

3.1. Maximizing the figure of merit

The Figure of Merit (FM) for optimizing experiments of this nature is defined as FM $\equiv P^2 I$, where P is the target polarization and I is the beam intensity.

From the above model, depolarization approximately scales with the beam intensity I,

$$P(I) = P_{max} - cI,$$

where c is a constant. Then one has $FM_{max} = (4/27c)P_{max}^3$ at $P(I) = \frac{2}{3}P_{max}$. The maximum of FM occurs when the depolarization is $\frac{1}{3}$ of its original value. Of course, when determining the optimal beam intensity, things other than FM have to be considered as well.

3.2. Minimizing the depolarization at constant beam intensity

The constant c in the above formulae is the depolarization at constant beam intensity, and can be minimized based on this model.

1. Depolarization is approximately inversely proportional to R_α. From Eq. (21), reducing the bead size is equivalent to increasing R_α. However, the concomitant reduction in channel size between beads mitigates this effect. It is known that the conductance of super fluid is reduced while the channel size is reduced [11]. Thus, the optimal bead size is a result of two competing effects. Published data [12] for a ^{3}He/^{4}He mixture at 0.5 K shows the change in achievable polarization with bead size, with and without beam.
2. Depolarization is also approximately inversely proportional to the raster area S_{ras}, which determines how soon the beam comes back to the same point. Increasing the raster area reduces the depolarization as well as the beam heating correction.

At a given beam intensity I (in units of C/s and $I \propto \dot{Q}(t_{pul}/t_{sep})S_{ras}$), S_{ras} and bead size, one can vary the variables t_{pul}, t_{sep} and instantaneous heating power $\dot{Q}$($\propto (I/d_f S_{beam})$) (where d_f is the duty cycle) to further minimize the depolarization, as long as $\dot{Q}(t_{pul}/t_{sep})$ remains constant. With the same initial 75% polarization, results for the NH_3 target in various cases are shown below, to be compared with the E143 case (75% → 67.7%):

1. Keep t_{pul} constant and vary t_{sep} (or $\dot{Q}$) by varying S_{beam}. Then t_{sep} changes according to: $t_{sep} = (t_{pul}/d_f)(S_{ras}/S_{beam})$. By doubling the beam spot area, it depolarizes to 67.9%. Increasing the beam spot area to the raster area (then raster becomes unnecessary), it depolarizes to 70.9% instead.
2. Keep t_{sep} constant and vary t_{pul} (or $\dot{Q}$) by varying d_f, according to $t_{pul} = t_{sep} d_f (S_{beam}/S_{ras})$. Reducing or increasing d_f by a factor of 20,[4] the depolarization does not change. The reason is obvious from Fig. 4, which shows that most of the time when the bead is at high temperature occurs after the beam pulse has gone, so it is the time after the beam pulse which dominates the temperature profile, and hence the polarization variation. In the case of E155, the bead will reach about the same maximum temperature after the beam pulse, because the same number of electrons will deposit the same amount of heat, and the heat removal in both cases is very small. Therefore, the temperature profile after the pulse will be almost identical in both cases, and hence the depolarization effect will be the same. However, when $d_f = 1$ (the continuous wave case), it only depolarizes to 70.7%.
3. Keep $\dot{Q}$ constant and vary t_{pul} (or t_{sep}).
   - This is relatively hard to do in the pulsed beam case at a fixed repetition rate, but still achievable by varying d_f and S_{beam}, while keeping the product constant. In this case,

[4] Similar to the conditions in SLAC experiment E155, which ran in early 1997.

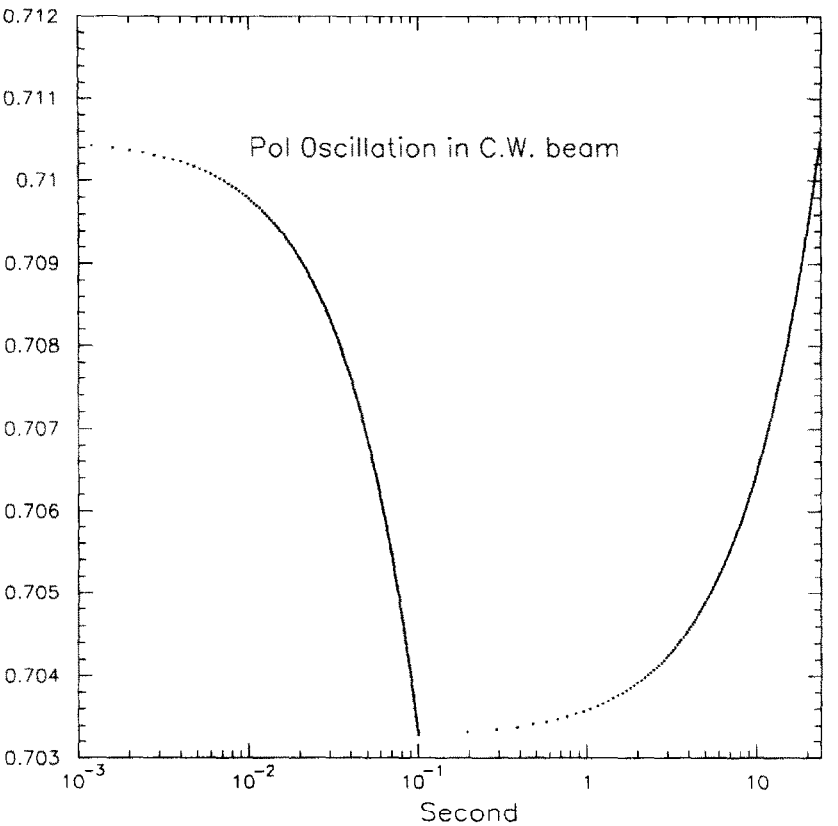

Fig. 8. NH_3 bead polarization oscillation in continuous wave beam, with raster frequency of 10 Hz.

$t_{pul} \propto 1/d_f$. The depolarization does not change much unless the changes are significant, as seen in the previous two cases, when changing d_f and S_{beam} separately.

- In the continuous wave case, it can be done simply by varying the amount of time spent at each raster position. In this case, the time scale for temperature rise in beam and its drop after the beam is gone is of the order of 10 ns. Calculations show that the depolarization is insensitive to raster frequencies between 10 and 1000 Hz, but the polarization oscillation grows larger with lower frequency, see Fig. 8. To avoid this, the raster frequency should be larger than 100 Hz. On the other hand, when the raster frequency is large enough to cut into the 10 ns time scale, the depolarization becomes smaller. At a frequency of 10^5 Hz, it only depolarizes to 72.0%. When the raster frequency goes to infinity, minimal depolarization occurs, decreasing to only 73.7% regardless of the beam size.

4. Conclusions

Due to the target depolarization from beam heating effects, the NMR measured target polarization can be larger than seen by the beam, and a correction must be made for this depolarization. This difference can be reduced by:

1. A larger raster area.
2. A different bead size.
3. A larger beam spot size.
4. Using continuous beam, with raster frequency ≥ 100 Hz.

Acknowledgements

This work was supported by Department of Energy Contract DEFG05-86ER40261 and the Institute of Nuclear and Particle Physics of the University of Virginia.

References

[1] A. Abragam, Principles of Nuclear Magnetism, Clarendon Press, Oxford, 1961.
[2] A. Abragam, M. Goldman, Rep. Progr. Phys. A 41 (1978).
[3] D.G. Crabb, W. Meyer, Ann. Rev. Nucl. Sci. (1997) to be published.
[4] K. Abe et al., SLAC E143, Phys. Rev. Lett. 74 (1995).
[5] K. Abe et al., SLAC E143, Phys. Rev. Lett. 75 (1995).
[6] D. Crabb, D. Day, Nucl. Instr. and Meth. A 356 (1995).
[7] G. Court et al., Nucl. Instr. and Meth. A 324 (1993).
[8] S.K. Dhawan et al., IEEE Trans. Nucl. Sci. NS-43 (1996).
[9] A. Thomas, Ph.D. Thesis, BONN-IR-94-15, Bonn University, 1994.
[10] Jr J.A. Katerberg, C.L. Reynolds, A.C. Anderson, Phys. Rev. B 16 (1977).
[11] H.A. Fairbank, J. Wilks, Proc. Roy. Soc. A 231 (1955).
[12] D.G. Crabb et al., in: W. Meyer (Ed.), Proc. 4th Int. Workshop on Polarized Target Materials, Bad Honnef, Germany, 1984.